Representation of vegetation and other nonerodible elements in aeolian shear stress partitioning models for predicting transport threshold

James King and William G. Nickling
Wind Erosion Laboratory, Department of Geography, University of Guelph, Guelph, Ontario, Canada

John A. Gillies
Particle Emissions Measurement Laboratory, Division of Atmospheric Sciences, Desert Research Institute, Reno, Nevada, USA

Received 23 December 2004; revised 6 September 2005; accepted 9 September 2005; published 1 December 2005.

[1] The presence of nonerodible elements is well understood to be a reducing factor for soil erosion by wind, but the limits of its protection of the surface and erosion threshold prediction are complicated by the varying geometry, spatial organization, and density of the elements. The predictive capabilities of the most recent models for estimating wind driven particle fluxes are reduced because of the poor representation of the effectiveness of vegetation to reduce wind erosion. Two approaches have been taken to account for roughness effects on sediment transport thresholds. Marticorena and Bergametti (1995) in their dust emission model parameterize the effect of roughness on threshold with the assumption that there is a relationship between roughness density and the aerodynamic roughness length of a surface. Raupach et al. (1993) offer a different approach based on physical modeling of wake development behind individual roughness elements and the partition of the surface stress and the total stress over a roughened surface. A comparison between the models shows the partitioning approach to be a good framework to explain the effect of roughness on entrainment of sediment by wind. Both models provided very good agreement for wind tunnel experiments using solid objects on a nonerodible surface. However, the Marticorena and Bergametti (1995) approach displays a scaling dependency when the difference between the roughness length of the surface and the overall roughness length is too great, while the Raupach et al. (1993) model's predictions perform better owing to the incorporation of the roughness geometry and the alterations to the flow they can cause.

Citation: King, J., W. G. Nickling, and J. A. Gillies (2005), Representation of vegetation and other nonerodible elements in aeolian shear stress partitioning models for predicting transport threshold, *J. Geophys. Res.*, *110*, F04015, doi:10.1029/2004JF000281.

1. Introduction

[2] Wind erosion is one of the major sources of mineral aerosols in the atmosphere [*Tegen et al.*, 2002] and the predictive capabilities of some of the most recent models for estimating the wind driven particle flux are limited by the misrepresentation of the effectiveness of vegetation to reduce wind erosion and dust emissions [*Gillies et al.*, 2002; *Minvielle et al.*, 2003]. The presence of nonerodible roughness elements (rocks, vegetation, etc.) on a surface is well understood to be an important factor in reducing soil erosion by wind. The limits of their protection of the surface, the understanding of the flow among the roughness elements and ultimately the erosion threshold prediction are complicated by the varying geometry, spatial organization and density of the roughness elements. The surface roughness in arid and semiarid environments consists of smooth soil or sand surfaces, nonerodible surfaces elements (large cobbles or boulders), and sparsely vegetated surfaces. The use of vegetation to reclaim large dust emitting areas suggests further emphasis needs to be placed on understanding how varying amounts of vegetation can provide protection from wind erosion. The development of a parameter to define the geometry and spatial organization of the elements that accounts for its influence on the aerodynamics of the airflow has proven difficult. The dimensionless ratio of the surface roughness density (λ, the total frontal area of all the elements to the total surface area) is the most prominent of the roughness parameters described in the literature but even it has shown to be insufficient when describing three-dimensional objects due to a bias inherent in using the front silhouette area [*Minvielle et al.*, 2003; *Musick et al.*, 1996].

[3] Two well-recognized models exist that predict the modified erosion threshold of a surface due to the presence

0148-0227/05/2004JF000281

of nonerodible roughness elements, however their relative performance through comparison with field and laboratory data has not been adequately undertaken. Approaches adopted from the meteorological research community to categorize the aerodynamics of closed canopy systems (e.g., roughness length) were initially extended to describe the flow characteristics over sparse vegetative communities to predict an erosion threshold. This approach was the basis for one of the first models to predict the protective role of roughness elements [*Lettau*, 1969] and accounts for roughness effects on wind erosion thresholds in a dust emissions model developed by *Marticorena and Bergametti* [1995]. The relationship between roughness length (Z_o), which is a measure of the magnitude of the aerodynamic drag on a surface using the ''law of the wall'', and surface roughness density (λ) provides a good descriptor of the flow at the top of the roughness over different densities, however it plays no role in furthering the knowledge of the potential surface emissions. *Marticorena and Bergametti* [1995] developed their model with the logarithmic profile theory [*Priestley*, 1959] but used the partition scheme of *Arya* [1975], which allocates the shear stress to the erodible surface and the roughness individually. This approach is based on the ratio between the surface roughness length (z_{oS}, associated with the surface between roughness elements) and the overall roughness length (Z_o, the roughness length that includes the influence of the surface and the roughness elements) to accommodate both practicality of measurement and simplification for application. This model has been utilized within larger-scale models [*Marticorena et al.*, 1997; *Zender et al.*, 2003] for estimating dust emissions at a continental scale, but no evaluation of its predictive capacity for vegetated surfaces has been performed, other than its initial derivation and comparison to the experimental data of *Marshall* [1971].

[4] Another approach developed to account for roughness effects on sediment transport threshold is to physically model wake development behind individual roughness elements. *Raupach* [1992] used this approach to develop a theory for the partitioning of the surface stress and the total stress over a roughened surface. This geometric and drag coefficient-based predictive model allows the user to specify available inputs to describe most environments and generate the ratio that characterizes the erosion threshold of an initially bare erodible surface with the threshold once nonerodible elements are present. This model, in the modified form presented by *Raupach et al.* [1993], and the model presented by *Marticorena and Bergametti* [1995] are critiqued in this paper.

[5] The objective of this paper is to compare the two threshold wind erosion models by evaluating their predictions of field and wind tunnel measurements with airflow over a range of roughness element scales, shapes, and distributions. Data sets reporting enough information to calculate results for both models provide an opportunity to contrast the weaknesses and strengths of the models. The background and assumptions of both models will be discussed to outline their theoretical and practical limitations followed by the direct comparison of the two models with the available data. Although these models only form one component of a complete dust emission model, the importance of roughness on the surface to control wind erosion is only second in importance to the ability of the soil surface to erode [*Tegen et al.*, 2002].

2. Background

2.1. Wind Profiles and Aerodynamic Roughness Parameters

[6] The bottom 10–15% portion of the boundary layer that develops over a surface is a characteristic of the roughness itself. This layer is typically described as two separate sublayers: an inertial sublayer and a roughness sublayer [*Panofsky and Townsend*, 1964; *Priestley*, 1959]. The inertial sublayer can be described by the logarithmic profile:

$$\frac{u_z}{u_*} = \frac{1}{\kappa} \ln\left(\frac{z}{Z_o}\right) \tag{1}$$

where u_z (m s^{-1}) is the mean wind speed at height z (m), κ is the von Karman constant equal to 0.4, u_* (m s^{-1}) is the shear velocity, and Z_o (m) is the roughness length. The logarithmic profile model is based on a steady two-dimensional motion over a plane surface where the flow is fully developed and turbulent with neutral stability.

[7] Surfaces with tall or significantly dense vegetation however, complicate the logarithmic profile by decreasing the depth to which equation (1) applies and changes the shape of the profile. The addition of a term in the logarithmic profile equation resolves this:

$$\frac{u_z}{u_*} = \frac{1}{\kappa} \ln\left(\frac{z-d}{Z_o}\right) \tag{2}$$

with Z_o representing the roughness length imposed by the roughness elements, and d representing the upward displacement of the mean momentum sink [*Jackson*, 1981]. The addition of d corrects the lower deviation of the logarithmic profile measured above a vegetated surface that is sufficiently dense. Z_o and d vary as a function of the height, spacing, shape of the elements, the wind direction and wind speed, depending on the local elevation changes created by the roughness elements and their flexibility [*Finnigan*, 1979; *Thom*, 1971]. In sparsely vegetated environments, it becomes difficult to theoretically apply d because of the heterogeneity of the instantaneous momentum sink level, which limits the application of the logarithmic profile model to define the vertical wind speed profile. The logarithmic profile can however represent wind speed profiles over a complex surface when temporally and spatial averaged measurements are used. This is rarely the procedure used in field experimentation and ignoring this requirement results in an incorrect estimate of the Z_o value (and/or d). Careful application of the logarithmic profile with critical understanding of its limitations can be accomplished providing a wide range of application for modeling purposes with the knowledge of surface roughness information from satellite imagery and a 10 m wind speed from a meteorological station [*Alfaro and Gomes*, 1995; *Shao and Leslie*, 1997].

[8] The layer typically below the mean momentum sink is termed the roughness sublayer and is influenced by the surface roughness elements and contains the characteristic

wake effects shed from the individual roughness elements. If the roughness is dense, the roughness sublayer has a spatially uniform flow characteristic but as the roughness becomes sparser, the heterogeneity of the roughness sublayer flow increases and consequently the surface shear stress increases [*Crawley and Nickling*, 2003]. This spectrum of shear stresses created between sparse and dense surface cover provides the theoretical basis for partition models and the major flow regimes discussed in section 2.2.

2.2. Flow Regimes

[9] Different flow regimes are created depending on element height, width, shape, spacing, and arrangement [*Lee and Soliman*, 1977; *Wolfe and Nickling*, 1993]. When a single element is inserted into a wind flow, a wake region develops downwind, in which the wind speed is sufficiently less than the averaged wind speed. The element sheds eddies, causing the flow in the wake to be separated from the surrounding flow. This wake region is synonymous with a sheltering (an area of no or reduced shear stress) provided by elements such as vegetation or rocks. A dimensionless number that reflects the effect of the roughness elements on the wind regime is the roughness density (λ):

$$\lambda = \frac{nbh}{S} \tag{3}$$

where n is the number of roughness elements of width b and height h per unit surface area (S).

[10] Skimming flow occurs when the wake region created in the wind flow behind an object is not allowed to develop. The other extreme case, isolated roughness flow, is where the wake created by the element fully develops before encountering other elements downwind. The intermediate case is when the wake region is somewhat imposed on the other elements: wake interference flow. These different flow regimes have been classified by a ratio of element spacing to height and plan view percent cover of the elements to the surface area [*Lee and Soliman*, 1977] which is positively correlated with the above aerodynamic properties only if the roughness is uniformly staggered and is regularly shaped (i.e., cubes, cylinders, etc.) (see review by *Wolfe and Nickling* [1993]).

2.3. Role of Sparse Vegetation in Sediment Entrainment and Transport

[11] In semiarid and arid environments vegetation is often spaced far enough apart [*Woodell et al.*, 1969] that the wake shed by an individual plant is allowed to fully develop or is only slightly obstructed by a downwind plant. This allows the averaged wind flow to not only penetrate the canopy but also exert forces on the surface, generally much greater in magnitude than to a surface without vegetation present. Sparsely vegetated surfaces produce two major effects on the wind regime: (1) an individual plant, because of its flexibility and porous nature, extracts momentum from the wind flow [*Gillies et al.*, 2002], and (2) it also forces the flow around the object creating local accelerations in the wind regime [*Glendening*, 1977]. These two effects work in opposition. The former contributes to the protection of the surface by damping the wind but the latter has the potential to enhance soil erosion by accelerating the local winds and increasing the total stress. The shape and spacing of elements modifies these effects based on the flow regimes discussed earlier.

[12] Two other roles of vegetation that influence the sediment transport system are its ability to trap moving sediment (reducing the horizontal flux and therefore reducing the vertical dust flux), and its occupation of a portion of the surface, thus offering a protective cover. Because of these effects a relationship between the threshold u_* and vegetation can be assumed to exist [*Raupach et al.*, 1993]. A quantitative description or map of the different amounts of vegetation and the effect they have on u_* and threshold u_* is a necessary input for predictive regional or even global dust emission models.

2.4. Shear Stress Partitioning

[13] The relationships that control dust emissions on bare surfaces and the reduction of sediment entrainment and transport on vegetated surfaces produces a complex theoretical and experimental problem. To understand this complete system of processes at the scale of a vegetation community, the components of these processes must be separately analyzed.

[14] A theoretical approach to describe this problem has been developed with ingenuity in the 1930s and experimental rigor in the 1970s. The work of *Schlichting* [1936] has been attributed to developing what is now known as drag partitioning. This theory states that the total drag on a roughened surface is the sum of the drag on the intervening surface and the drag on all of the individual roughness elements on that surface [*Schlichting*, 1936].

[15] This partition concept was applied in the context of vegetation and soil erosion by wind in the experiments performed by *Marshall* [1971]. This extensive laboratory work established that the partition was mostly dependent on λ and only slightly dependent on the shape and arrangement of the roughness elements [*Marshall*, 1971]. Lambda defines the element density in terms of spacing and size to allow for predictability through the development of theoretical models. The roughness density however, cannot explain the dynamic response of the wind to this type of roughness completely. Because of the natural variation in both vegetation and other nonerodible elements a distribution of the variables in equation (3) creates a local distribution of roughness densities. This variation cannot be properly explained by the averaging effect of totaling the geometric properties of the elements over the total surface area in equation (3), producing an inherent bias in the grid size chosen for modeling natural landscapes [*MacKinnon et al.*, 2004]. In addition, arid environments frequently exhibit vegetation growing on top of dunes (nabkhas or coppice dunes) or two different types of vegetation growing within one another with different geometric properties creating a three-dimensional distribution that λ would represent inadequately. Last, researchers have sought an additional term or terms to describe the porosity of vegetation and its effect on the frontal area based roughness concentration [*Minvielle et al.*, 2003; *Musick et al.*, 1996]. However, the effect of vegetation has been shown to create different wake characteristics due to the through flow of air as well as its flexibility that increases its effectiveness to absorb

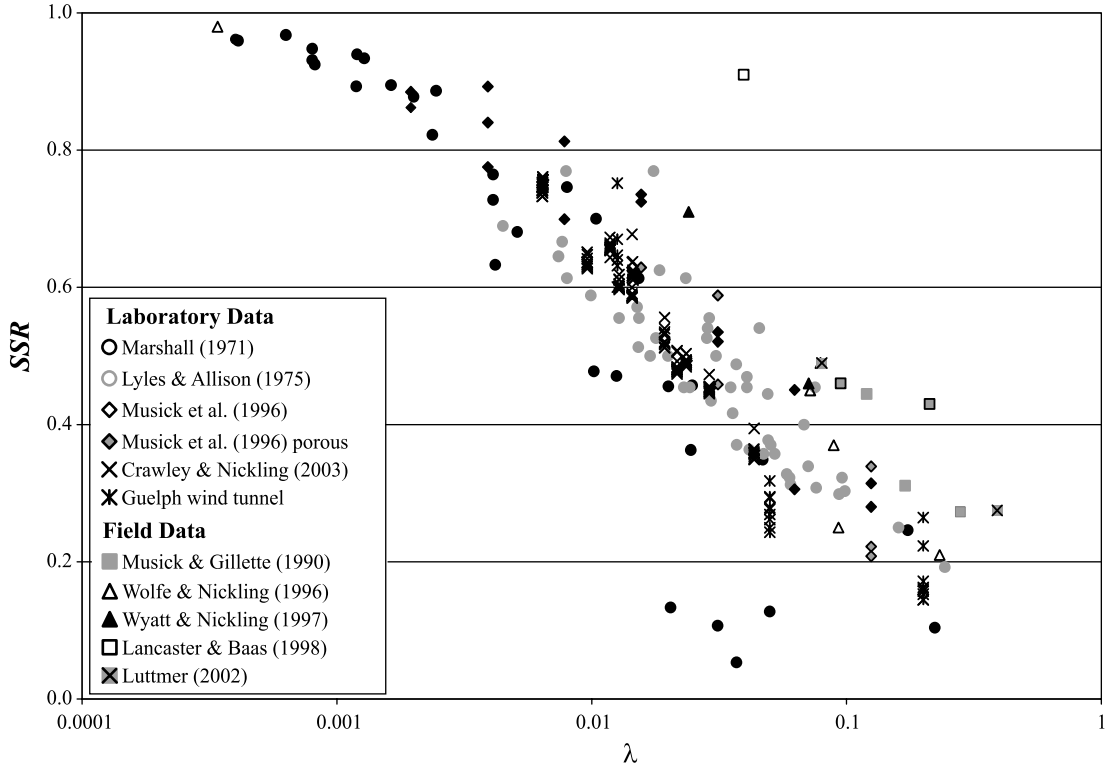

Figure 1. Shear stress ratio plotted against λ for available field and laboratory data.

momentum compared to a solid object with an equivalent frontal area [*Gillies et al.*, 2002].

[16] Although widely adopted, λ as defined in equation (3) does not fully describe the effect that roughness can have on airflow toward the surface. This creates a problem when comparing the performance of wind erosion models as they use equation (3) as an independent variable for roughness. Nevertheless, the difference between the two models discussed in this paper resides in their theoretical approaches and applications of λ, which they both utilize as the surface roughness descriptor. The comparisons made use of the same data sets to minimize the inherent bias in this variable.

3. Model Evaluation

3.1. *Raupach* [1992] and *Raupach et al.* [1993] Model

[17] The basic understanding of the dynamic relationship between shear stress and vegetation density led *Raupach* [1992] to develop his theoretical shear stress partitioning model. This model defines the partition of drag in terms of a shear stress ratio (SSR) of the shear stress threshold for sediment entrainment for the bare erodible surface in question (τ_s) to the total shear stress threshold of the surface including roughness (τ). The model is expressed as

$$R_t = \left(\frac{u_{*S}}{u_*}\right) = \left(\frac{\tau_S}{\tau}\right)^{1/2} = \left(\frac{1}{(1+\beta\lambda)}\right)^{1/2} \tag{4}$$

where β is defined as the ratio of the drag coefficient of single roughness element to that of the surface without elements (C_R/C_S). In this approach, β accounts for the shape of the elements and controls the partition of the drag [*Raupach*, 1992]. The performance of this approach is visible in the collected data sets of measured R_t collapsing when graphed against λ (Figure 1). Despite this performance, the model was found by *Raupach et al.* [1993] to be less than adequate when validated against laboratory and field results. One of the reasons suggested for this was that there was an aspect ratio dependency not directly included in the model [*Raupach et al.*, 1993].

[18] To address the identified shortcomings in equation (4), *Raupach et al.* [1993] modified the model by adding two terms; the first defines an aspect ratio while the other delineates the threshold of the surface by some function of the maximum stress (τ_s'') instead of the average stress [*Raupach et al.*, 1993]. This redefinition is essential in the context of soil erosion and dust emission as the threshold of a surface is not a function of an averaged stress but a maximum stress [*Stout and Zobeck*, 1997]. *Raupach et al.* [1993] incorporates these terms by expanding the *Raupach* [1992] form to

$$R_t'' = \left(\frac{\tau_S''}{\tau}\right)^{1/2} = \left(\frac{1}{(1-m\sigma\lambda)(1+m\beta\lambda)}\right)^{1/2} \tag{5}$$

where σ is defined as the ratio of the basal to frontal area and m is a parameter between 0 and 1 that accounts for the spatial and temporal variations in the stress on the intervening surface. *Raupach et al.* [1993] suggests a value of 0.5 for m for a flat, erodible surface and a value that approaches one for an erodible surface that is quasi-stable with equilibrium bed topography.

[19] One of the main assumptions in the *Raupach* [1992] and *Raupach et al.* [1993] approach is that the roughness is modeled as a solid object. This assumption allows for the

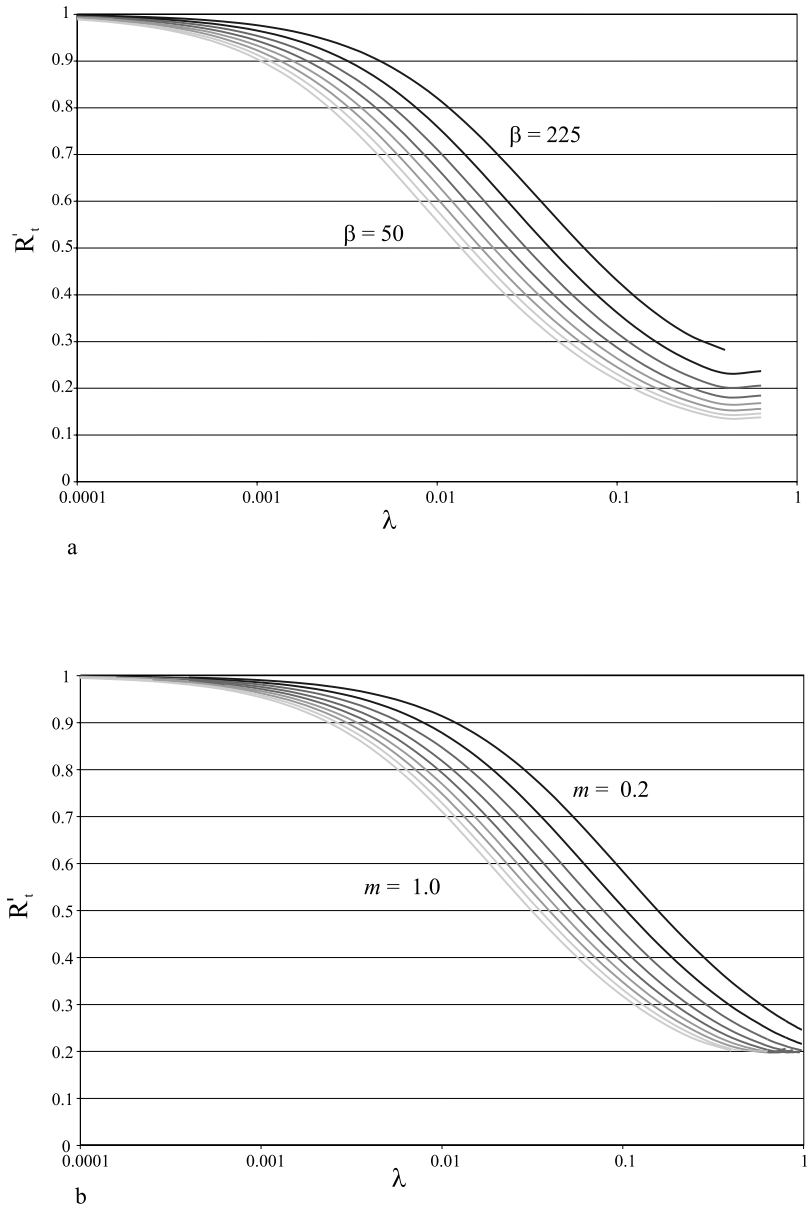

Figure 2. R_t' plotted against λ showing the influence of β and m. (a) Variation of β from 50 to 225 in 25 increments. (b) Variation in m from a value of 0.2 up to 1.0.

further simplification of the drag reduction behind an individual roughness element because it expresses an area with no stress and over the rest of the surface, a time-averaged uniform stress. However, behind a solid object there is a gradient of drag reduction that is continually changing in both time and space. Additionally, when an element is porous the reduction of drag will unlikely be completely reduced to zero behind an individual object and will also vary temporally and spatially [*Musick et al.*, 1996]. These variations will depend on the porosity of the objects as well as the other variables already incorporated into the model.

[20] Because of the complex interactions within a sparse canopy a model that could predict the threshold of entrainment within such a landscape would provide an invaluable resource for application in regional dust models and global circulation models (GCMs). Assumptions made in the theoretical model of *Raupach et al.* [1993] appear to limit its applicability, however recent investigations have shown that its correlation to both laboratory and field shear stress partitioning data is very high [*Crawley*, 2000; *Gillies et al.*, 2000; *Musick et al.*, 1996; *Wyatt and Nickling*, 1997]. This may be due to two important factors, the approximations of the β and the m parameter. The β parameter is difficult to measure in a field setting due to the complications of measuring the drag coefficient of a surface without the influence of the vegetation over the range of wind speeds required. Attempts with small wind tunnels [e.g., *Gillette and Stockton*, 1989] have previously been made to measure this variable within the vegetation, but it is questionable

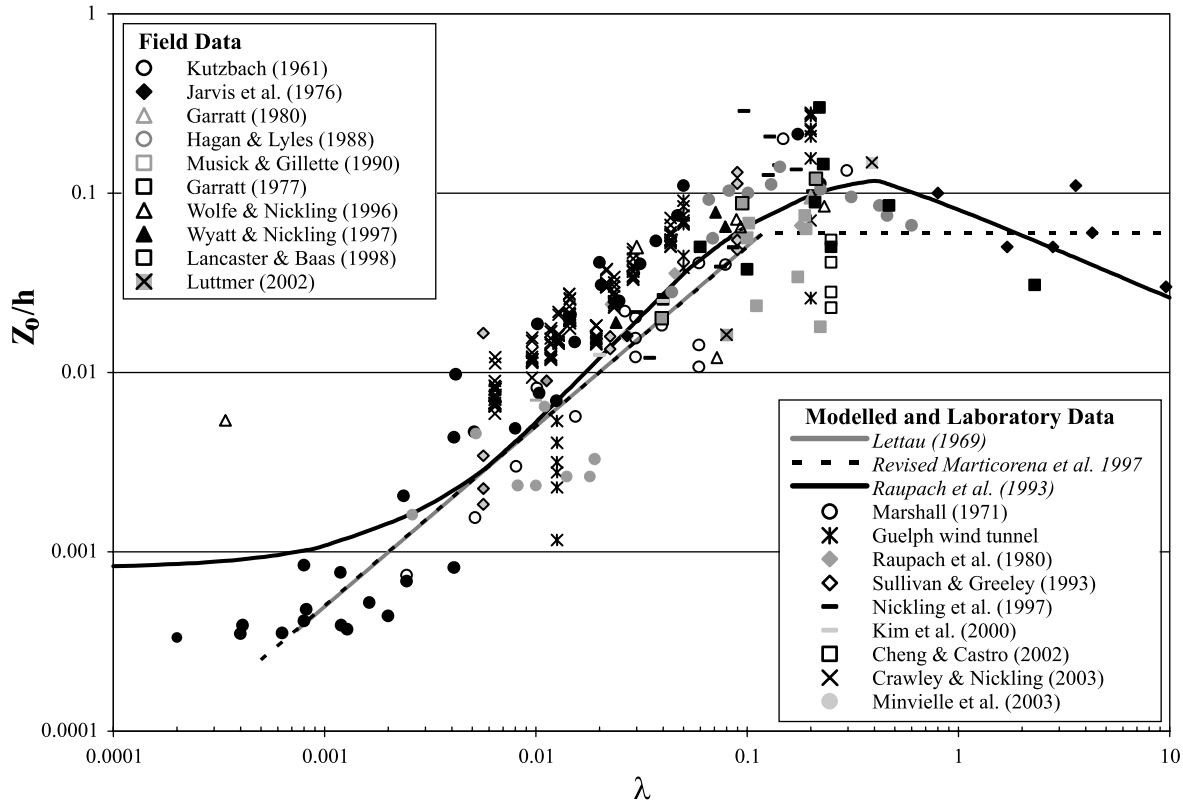

Figure 3. Z_o/h plotted against λ for field and laboratory data as well as the relationships suggested by *Lettau* [1969], *Marticorena and Bergametti* [1995], and *Raupach et al.* [1993].

whether the boundary layer created by this type of tunnel represents the same effect on the surface as that produced by the atmospheric boundary layer and may only allow a threshold wind speed to be determined. More recent attempts in measuring the drag coefficient of the surface through the use of Irwin sensors and drag plates on similar landscapes without vegetation has provided more representational results by allowing in situ measurements within natural wind conditions [*Gillies et al.*, 2000; *Wyatt and Nickling*, 1997]. The other half of the β parameter, the drag coefficient of a single roughness element, has been recently shown to vary considerably for the range of Reynolds numbers found in a field setting for moderately flexible vegetation [*Gillies et al.*, 2002]. This increases the drag coefficient of the roughness and makes it a function of wind speed, which increases the error when assuming a value of a solid object for porous vegetation. Since the β parameter is a dominating value in the *Raupach et al.* [1993] model, its approximation can lead to a gross overestimation or underestimation of the threshold ratio (Figure 2a).

[21] The m parameter is as dominating as the β parameter because it is a multiplier of both the β and σ term and has a value ranging between 0 and 1 as defined by *Raupach et al.* [1993] (Figure 2b). According to *Raupach et al.* [1993], its value represents the difference between the average and maximum shear stress value found on the intervening surface. Evaluation of this difference has been limited to estimations on timescales of 5 min over an unlimited fetch due to instrument limitations [*Wyatt and Nickling*, 1997], however it has been measured recently through new instrumentation at time intervals of 1 Hz and over the complete surface [*Crawley and Nickling*, 2003]. The data of *Crawley and Nickling* [2003] have shown that the difference between τ_s'' and τ_s' is a simple multiple but not directly correlated to the m parameter as stated by *Raupach et al.* [1993]. However, this relationship still needs to be confirmed for both porous and solid roughness elements. As the m parameter attempts to account for the nonuniformity of the surface stress, accounting for its effect on the erosion threshold of an erodible surface is crucial. Therefore an error in the estimation of this parameter could also result in large errors in R_t (Figure 2b).

[22] The overall performance of this model and particularly its predictive capability as compared to that of the *Marticorena and Bergametti* [1995] model is discussed in section 3.5 to explore the differences between these drag partition-based models.

3.2. *Marticorena and Bergametti* [1995] Model

[23] This model was developed partially on the observed relationship between Z_o of a roughened surface and λ derived through wind tunnel and field experiments (Figure 3). This extensive collection of both field and wind tunnel experiments covers the range of flow regimes discussed in section 2.2 very well. From a λ of 10^{-4} to 10^{-1} an obvious increase in the ratio of Z_o to mean roughness height (h) occurs at the merging of isolated roughness flow and wake interference flow regimes. Continuing toward a more densely populated roughness, the occurrence of skimming flow coincides with the leveling of the values and the eventual decrease in Z_o/h.

This pattern is also well described by the *Raupach* [1992] model for a solution of Z_o/h as illustrated in Figure 3. *Marticorena et al.* [1997] define a similar curve, although its definition is presently reconfigured due to a calculation error identified in the work of *Marticorena and Bergametti* [1995] (B. Marticorena, personal communication, 2003) concerning the *Marshall* [1971] data set (see Appendix A). However, the model defined by *Lettau* [1969] for λ below 10^{-1} can be substituted to closely approximate this range of the *Marshall* [1971] data set, which was the source of error in the work by *Marticorena and Bergametti* [1995] and *Marticorena et al.* [1997]. This relationship between Z_o/h and λ (Figure 3) displays the dependence of the former variable on the latter, furthering its credibility as a measurement for surface roughness. *Marticorena and Bergametti*'s [1995] partition scheme utilizes Z_o values associated with surfaces of a specific roughness character that have been published in the literature. The origin of their partition scheme and the effect it has on model estimates of the threshold ratios are discussed below. The previously mentioned calculation error made by *Marticorena and Bergametti* [1995] was corrected for all further analysis.

[24] *Arya* [1975], using logarithmic profile theory developed a model that is based on the assumption that equilibrium profiles will develop over a roughened surface as well as the smooth surface between the roughness elements. *Marticorena and Bergametti* [1995] adopted this approach while incorporating a fixed value for the downwind distance over which the two profiles (one over the entire surface and the other an individual roughness element along the surface) equate. *Alfaro and Gomes* [1995] made measurements of the shear velocity downwind from a roughness element showing that this value varied with different roughness types. This is due to the fact that the wake development behind an obstacle is dependent on the roughness height and spacing as defined by *Coles*' [1956] wake law. By using a fixed value rather than a roughness-specific value for the downwind distance at which the two profiles equate, the *Marticorena and Bergametti* [1995] model requires fewer inputs and calculations, furthering its ease of use while limiting its applicability.

[25] Starting with equation (1) with Z_o defined as the roughness length of the surface including the roughness and u_* defined as the overall shear velocity, a second logarithmic law is assumed for the surface on which the roughness elements reside and has the form:

$$\frac{u_z}{u_{*S}} = \frac{1}{\kappa} \ln\left(\frac{z}{z_{oS}}\right) \tag{6}$$

where u_{*S} (m s^{-1}) is the small-scale shear velocity and related to the local shear stress by the relationship $\tau_s = \rho_a (u_{*S})^2$, and z_{oS} (m) is the local roughness length of the intervening surface with an internal boundary layer (IBL) of height δ (m). This layer is assumed to develop behind each individual roughness element and reaches the form of equation (6) when equilibrium has been established between the IBL and the region above it, where equation (1) applies (when the lowest u_z of equation (1) equals u_z at height δ of equation (6)) [*Arya*, 1975]. Arranging these two equations into the drag partition form of a ratio of the surface stress and total stress, gives:

$$\frac{\tau_s}{\tau} = \left(\frac{u_{*S}}{u_*}\right)^2 = \left(\frac{\ln\left(\delta/Z_o\right)}{\ln\left(\delta/z_{oS}\right)}\right)^2 \tag{7}$$

or

$$\frac{\tau_s}{\tau} = \left(\frac{u_{*S}}{u_*}\right)^2 = \left(1 - \frac{\ln\left(Z_o/z_{oS}\right)}{\ln\left(\delta/z_{oS}\right)}\right)^2 \tag{8}$$

[26] From equation (8) the only variable not yet defined is δ, which has been related to the boundary layer development for a step change in roughness, which has been investigated thoroughly and modeled by *Elliot* [1958] as

$$\ln\left(\frac{\delta}{z_{oS}}\right) = a\left(\frac{x}{z_{oS}}\right)^{0.8} \tag{9}$$

$$a = 0.75 - 0.03 \ln\left(\frac{Z_0}{z_{oS}}\right) \tag{10}$$

where a is a function of the roughness density and flow properties and x (cm) is the distance downwind from an individual roughness element. *Arya* [1975] in his study of SSR equates the left side of equation (9) to a function of z_{oS}, λ, and separated flow length. *Marticorena and Bergametti* [1995], however, further simplify equation (9) by assuming a length of 10 cm for x. *Marticorena and Bergametti* [1995] also adopt the value of $a = 0.35$ from the wind tunnel study of *Pendergrass and Arya* [1984]. Because of the above mentioned miscalculation of the *Marshall* [1971] data set, the authors of this paper propose a new value of a equal to 0.7, which is the average value for the *Marshall* [1971] data from the proposed solution of the variable a by *Elliott* [1958] in equation (10) (Appendix A). This value produces very good agreement with the *Marshall* [1971] data set and the revised model's performance will be analyzed in the next section.

[27] The simplification of equations (9) and (10) theoretically limits the range of roughness concentrations as well as the type of roughness elements that the model can represent adequately. This downwind distance value of 10 cm has only been investigated at scales associated with wind tunnels and was calculated due to its agreement with the *Marshall* [1971] data set [*Marticorena and Bergametti*, 1995]. This potentially limits the application of the model to only small-scale wakes, as this parameter is not independently scaled to the object size but an absolute distance. Furthermore, this distance is only for solid objects for which a downwind wake develops closer to the object than if the object was porous [*Castro*, 1971].

[28] The final form of the partition model becomes

$$f_{eff} = \frac{u_{*S}}{u_*} = 1 - \frac{\ln\left(Z_o \Big/ z_{oS}\right)}{\ln\left(0.7\left(10 \Big/ z_{oS}\right)^{0.8}\right)} \qquad (11)$$

with the units of Z_o and z_{oS} being in centimeters. The advantage of this approach for drag partitioning is that Z_o describes the roughness in a manner similar to the drag coefficient (but height independent) when the sublayer is defined by the surface scale [*Marticorena and Bergametti*, 1995]. This approach assumes a minimum fetch for the internal boundary layer to develop which will correspond to the maximum height of the roughness. Natural variations in height produce a bias that cannot be accounted for by a roughness length inferred from average roughness density measurements because a local increase in roughness density will contribute more to the roughness length value than its apparent fraction [*Wieringa*, 1993]. Although *Marticorena and Bergametti* [1995] include this in their assumption, they provide no direct solution for identifying the overestimation of the measured Z_o for natural surfaces.

[29] *Marticorena et al.* [1997] provide an addition to equation (11) for surfaces that exhibit two distinct surface roughness scales not including the erodible surface itself. This double-drag partition is quantified by multiplying two partition equations with one expressing the reduction from the most frequent roughness to the surface and the other between the most frequent roughness and the interspersed larger-scale roughness as a function of the distance separating them [*Marticorena et al.*, 1997].

3.3. Selected Data Sets

[30] The data sets chosen for this analysis were the only ones known to the authors where both models could be correctly calculated and where the SSR was measured during the experiment. Furthermore, the methodology implemented by these studies allowed for a high certainty in their declared values as all measured quantities were reported with ample sampling numbers and averaging periods. Figures 1 and 3 show that many experiments which either reported Z_o or R'_t have been published, however only five could be utilized due to the above stated requirements.

[31] Of the data sets presented, the wind tunnel data from *Marshall* [1971] (using wooden cylinders on a plywood floor) provide independently measured stresses on the roughness and the floor using drag balance equipment. Z_o values were calculated based on free stream values of 20.3 m s^{-1} measured at 0.28 m for surfaces with roughness elements and 0.046 m for the surface without any roughness elements [*Marshall*, 1971]. The data of *Crawley and Nickling* [2003] were similar but used Styrofoam cylinders mounted on a smooth plywood surface with drag balance equipment to measure element drag. Z_o values for the roughened surfaces tested by *Crawley and Nickling* [2003] are calculated based on the measured free stream wind velocity. The values for the drag coefficients of the surface were measured in situ by the drag meters used in the study while the drag coefficient of the elements used was 0.3 as suggested by *Taylor* [1988] for a cylinder. *Crawley and Nickling* [2003] also calculated the maximum surface shear stress values using Irwin sensors, which are used to calculate the maximum SSR, defined as the maximum surface shear stress divided by the average total shear stress. The aerodynamic roughness of the same plywood surface used by *Crawley and Nickling* [2003] as well as surface shear stresses of three surfaces of increasing roughness were measured in a different study by the authors labeled as Guelph Wind Tunnel (GWT), which will be described elsewhere. The roughness elements used in the GWT experiment consisted of wooden cubes in a staggered array at three different roughness densities. The additional Irwin sensor data are part of a larger data set (to be published elsewhere) and are used in the present study to compliment the SSR data obtained from the literature. SSR values in the GWT data set were calculated from vertical wind profiles and Irwin sensor measurements (averages and maximums) made at the surface. Z_o was deduced from the vertical wind speed profile measurements over the roughened surfaces and z_{oS} from profile measurements over the wind tunnel floor in the absence of the roughness elements. The surface drag coefficient utilized for the GWT study was calculated from Pitot tube measurements over the bare surface and an element surface drag coefficient was assigned a value of 1.05 from independent measurements giving a value of $\beta = 263$.

[32] The remaining four data sets are field experiments made on erodible surfaces with naturally occurring boundary layer flows. The *Lancaster and Baas* [1998] and *Luttmer* [2002] data sets are from experiments conducted at Owens Lake, California, on sandy surfaces with different amounts of salt grass (*Distichlis spicata*) cover and one complimentary bare site. For the *Lancaster and Baas* [1998] data the SSR values were calculated based on the threshold u_* required for the bare site and the u_* measured at the vegetated sites with an anemometer tower (based on one hour averages); the threshold of sand transport was detected by a Sensit (piezoelectric sensor device) [*Lancaster and Baas*, 1998]. The Z_o values for the sparsely vegetated surface were taken directly from *Lancaster and Baas*' [1998] published values. Their z_{oS} value for the bare surface was used to calculate the surface drag coefficient [*Lancaster and Baas*, 1998]. The data from *Luttmer* [2002] consisted of two vegetated sites where vertical wind speed profiles provided Z_o and u_* values while the measurement provided by Irwin sensors gave surface u_* values. The z_{oS} values were also assumed to be the same as the Z_o value obtained over the bare surface used in her experiment, which was also used to calculate the surface drag coefficient. The roughness drag coefficient used for both of these studies was obtained from *Nickling et al.* [1999] where drag coefficients of varying thickness of salt grass were calculated using force balances in a wind tunnel resulting in β values of 74 and 72 for *Lancaster and Baas* [1998] and *Luttmer* [2002], respectively.

[33] The data of *Wyatt and Nickling* [1997] are from measurements over three vegetated sites populated by creosote (*Larrea tridentata*) and bursage (*Ambrosia duinosa*) and one bare site on the El Dorado playa in southern Nevada. SSR values were estimated from the total

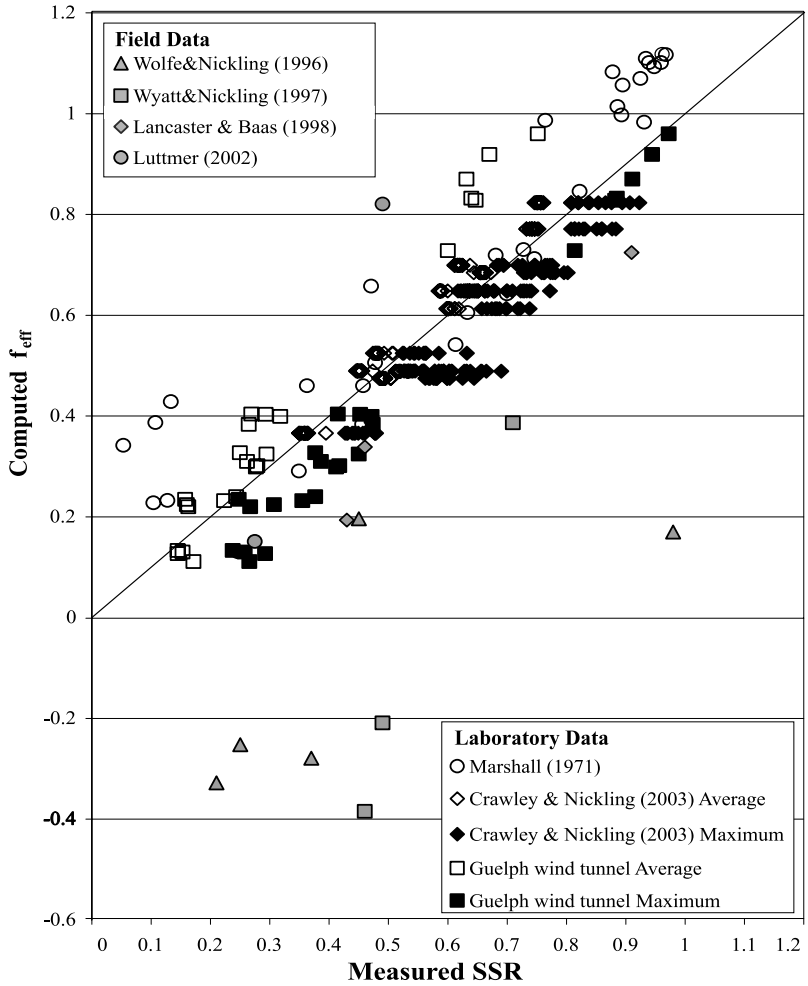

Figure 4. Field and laboratory data plotted as measured SSR against the modeled f_{eff} value as predicted by the *Marticorena and Bergametti* [1995] model.

u_* determined from wind speed profile data obtained with a 10 m tower with cup anemometers (based on 10 min averages) and measurements of the surface u_* obtained using Irwin sensors. Z_o was calculated on the basis of published values of Z_o/h and the mean shrub height presented in Table 1 of *Wyatt and Nickling* [1997], whereas the z_{oS} for all three vegetated sites was assumed to be equal to the average Z_o measured at the bare site. The value given for $\beta = 202$ was derived from the surface mounted creosote bush in the experiment on a playa for the drag coefficient of the object while the surface drag coefficient was from tower measurements over a bare playa surface [*Wyatt and Nickling*, 1997].

[34] The last set of data was obtained from *Wolfe and Nickling* [1996] for five sparsely vegetated sites in the Sonoran Desert, Arizona. The type of vegetation at their sites varied but included creosote, bursage and the sparsest site was populated with mesquite (*Prosopis glandulosa*) [*Wolfe and Nickling*, 1996]. A field wind tunnel was utilized to calculate z_{oS} and threshold u_* for the surface between the vegetative roughness elements while the total u_* and Z_o were derived from measurements of 15 min average wind speeds collected by anemometers on a 10 m anemometer tower and applying the logarithmic profile model [*Wolfe and Nickling*, 1996]. Surface drag coefficients were obtained from wind tunnel tests in situ while the roughness drag coefficient used was from the findings of *Wyatt and Nickling* [1997], giving values of β from 95 to 204.

[35] The *Marticorena and Bergametti* [1995] f_{eff} calculated for the data sets is plotted against the measured SSR for both wind tunnel and field investigations in Figure 4. The same data sets are shown in Figure 5 but plotted with R_t' calculated by the *Raupach et al.* [1993] model.

3.4. *Marticorena and Bergametti* [1995] Model Performance

[36] The data presented in Figure 4 show very good agreement with equation (11) for the experiments conducted in laboratory wind tunnels ($R^2 = 0.91$ with a forced zeroed intercept) with a slight overestimate (slope of 1.07 and a standard error of 0.07) based on the averaged measured values. The maximum SSR values (Figure 4) show that the revised model of *Marticorena and Bergametti* [1995] represents a value in between the average and maximum measured ratio. This becomes a very useful function as it has been shown that the average shear stress at the surface is not the driving force for sediment movement

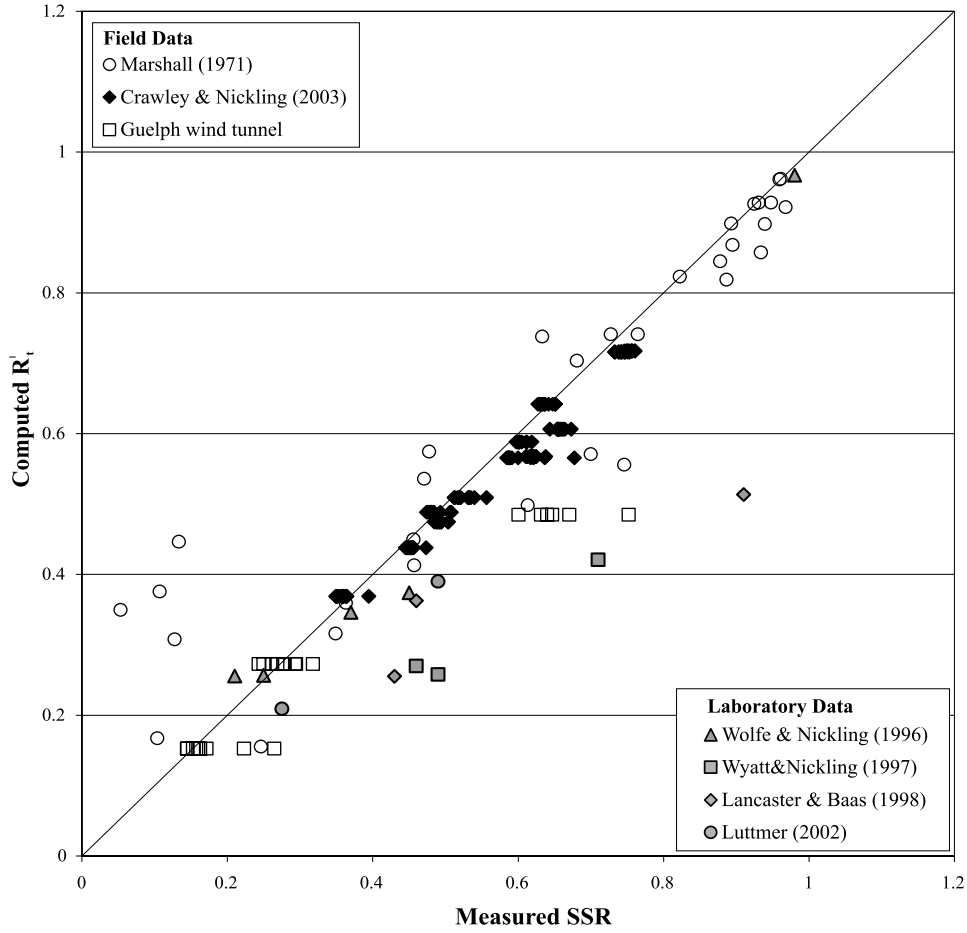

Figure 5. Field and laboratory data plotted as measured SSR against the modeled *Rt* value as predicted by the *Raupach et al.* [1993] model.

but some function of the maximum [*Gillette et al.*, 1996]. However, the four field experiments plotted in Figure 4 do not agree well with the model. This implies that the model may not be able to be extended into field environments, which could be due to the poor representation of the surface roughness configurations by Z_o values as discussed in section 3.2. The data of *Lancaster and Baas* [1998] and *Luttmer* [2002] perform the best while the data of the other two studies result in five of the eight values being negative. Although the original definition of the *Marticorena and Bergametti* [1995] model limits its application to roughness densities less than $\lambda = 0.05$, the performance of the model to predict these data appears to be independent of the roughness density as the GWT data set has roughness density values of 0.2, which are well predicted. Additionally, the data sets of *Luttmer* [2002] and *Lancaster and Baas* [1998] also seem to be well predicted even though their roughness densities are 0.08, 0.39 and 0.04, 0.09, and 0.21 respectively.

[37] Several reasons that may account for the poor performance of the model for the field data include (1) using z_{oS} of the bare surface control site to represent the surface of the natural sites with vegetation, (2) the Z_o values published are overestimated compared to local surface concentrations because of the natural variability of the vegetation and the subsequent increase in the measured Z_o as discussed previously, and/or (3) the inability of the model to incorporate the effects of the vegetation on wind flow in natural environments because of the large difference in the roughness scale of the surface and the vegetation.

[38] The first reason given is plausible, although the values utilized from *Wolfe and Nickling* [1996] were directly obtained by a field wind tunnel, while the value obtained for *Lancaster and Baas* [1998] and *Wyatt and Nickling* [1997] were inferred from neighboring sites using a 10 m anemometer tower (and in the case of *Lancaster and Baas* [1998] they were from actual threshold measurements). Furthermore, the sensitivity of the model to changes in z_{oS} is low, only producing a change of 10% in the calculated f_{eff} value with a 20% increase. Even with an increase by 200% of the field measured z_{oS} values, the regression coefficient only increases by 1% for the entire data set.

[39] As stated by *Wieringa* [1993], an apparent increase in Z_o will be measured over a nonuniform array due to the dominating effect of a local increase in roughness density. *Taylor* [1988] also argues that for turbulent length scales over nonuniform roughness concentrations, the integrative value of a grid scaled area is higher than the surface average. Since this affects Z_o (in the numerator of equation (11)) by making it larger without changing the

value of any of the other variables, the resulting f_{eff} value will decrease. Although no consistent increase has been reported for a given standard deviation in roughness density, it is unlikely that the poorly modeled results of the field data are likely due to this apparent increase, given the good agreement between the wind tunnel and model results.

[40] The simplified approach of *Marticorena and Bergametti* [1995] in comparison to the original derivation by *Arya* [1975] may have led to a scaling issue between the Z_o produced by sparse natural vegetation and that of an erodible surface. The addition of a double-partition approach by *Marticorena et al.* [1997] is noted; however, in the field experiment data utilized for this comparison, only one scale of roughness is present for the majority of sites (the exception is two sites from *Wolfe and Nickling* [1996] that contained both bursage and creosote, but not enough information was published to calculate the double-partition equation). The superior estimation of the *Lancaster and Baas* [1998] and *Luttmer* [2002] data by the *Marticorena and Bergametti* [1995] model emphasizes this scaling issue because the roughness in these cases were much closer in scale to the roughness of the erodible surface (salt grass with a mean height of 0.10 m) in comparison to the creosote-dominated landscapes of *Wolfe and Nickling* [1996] and *Wyatt and Nickling* [1997] (mean height of 1.02 m and 0.97 m, respectively).

[41] This difference of scales suggests the need for incorporating a displacement height requirement into the model to account for this difference. A displacement height of zero was utilized for both sets of data measured over creosote by *Wolfe and Nickling* [1996]. A breakdown in the assumptions of the logarithmic profile approach may be the reason for the scaling issue because of the variability of the flow field over sparse roughness elements. Although these data were averaged temporally, only one anemometer tower was utilized to obtain these results. To satisfy the assumptions of the logarithmic profile a spatial average might be required in addition to a temporal average due to the local variability in the flow field.

3.5. *Raupach et al.* [1993] Model Performance

[42] The performance of the *Raupach et al.* [1993] model using equation (5) with $m = 1$ is very good ($R^2 = 0.86$ for all of the data plotted and $R^2 = 0.89$ for wind tunnel only data, both with a forced zero regression) and produces only a slight underestimate (slope = 0.94 and a standard error of 0.07) of the measured data overall (Figure 5). There is no significant difference between the prediction with or without inclusion of the field data, however the field data are consistently underestimated in comparison to data obtained from laboratory wind tunnel studies.

[43] The general underestimation can be due to a misrepresentation of drag coefficients for vegetation used in the β parameter, but commonly the errors associated with this term will decrease the value of β and therefore increase the modeled value of the stress partition. The drag coefficient of the surface is height-dependent and in most cases it is taken at the height or at 1.5 times the height of the roughness (for laboratory wind tunnel simulations), but this is not always the case and not always theoretically correct for field scale vegetation. *Raupach* [1992] does not specify a height at which β should be calculated. If it is calculated for a height that is too low in comparison to the heights over which u_* has been calculated it leads to a larger surface drag and therefore a smaller final R_t'. In addition, the drag coefficient for the roughness itself is typically underestimated by substituting a solid element coefficient for a porous object. However, in the case of all three of the field studies analyzed here, actual drag coefficients were utilized – minimizing the error associated with this portion of the model.

[44] Although a value of $m = 1$ is not suggested by *Raupach et al.* [1993] for erodible surfaces (equation (5)), they also define the SSR based on averaged surface shear stresses with $m = 1$. The modeled values compared in this study were calculated only using averaged measured SSR values, making this approach suitable to the original model definition. Additionally, the values of m suggested by others through experimental work has shown that no consistent value is suitable for most surfaces as solved for in equation (5) and that the original definition of this parameter is incorrect [*Crawley and Nickling*, 2003]. Therefore it is problematic to assume or calculate the value of m for the presented data sets based on its original definition. The value of $m = 1$ allows a restriction of the model's performance but does not directly contradict the findings presented in the literature.

[45] It is possible that another scaling term or modification of the m parameter needs to be incorporated into the model to reduce the apparent overestimation of R_t'. This scaling parameter needs to be associated with the length scales of the roughness elements in order to adjust correctly for the increased shear stress reduction of taller objects in addition to the height to width ratio already included in equation (5). Formulation of such a scaling parameter should be considered an important area of future research.

[46] Although both values calculated in Figure 5 represent an average value, it is known that the temporally averaged value of surface shear stress is not normally distributed and that a maximum value describes the erosion potential of the surface more successfully. The *Raupach et al.* [1993] model was used with a value of $m = 1$ for this study due to its inability to be successfully estimated a priori, reducing the importance of a direct comparison. However, the importance of using a maximum surface stress measurement over an averaged one may explain the difference between the estimation of uniform arrays of roughness (wind tunnel experiments) and the nonuniform arrays of porous objects found in the field experiments.

4. Conclusions

[47] The comparison between the models of *Raupach et al.* [1993] and *Marticorena and Bergametti* [1995] has shown the potential of the partitioning approach to wind erosion on roughened surfaces to be a good framework in which to explain the effect of roughness on entrainment (and potentially transport) of sediment by wind. Both models provided very good agreement for the wind tunnel experiments using solid objects on a nonerodible surface,

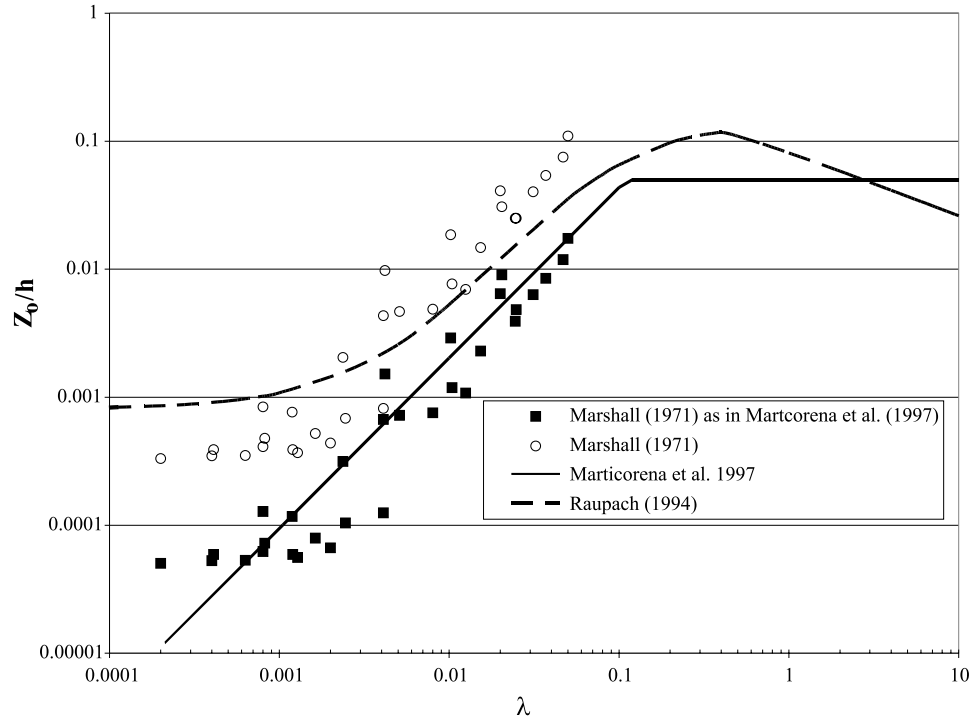

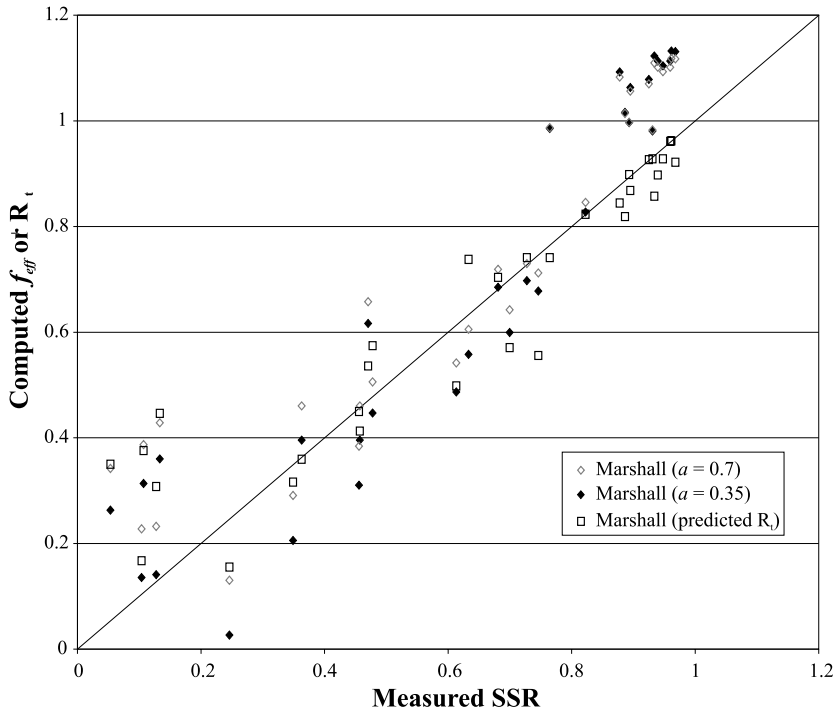

Figure A1. (top) *Marshall* [1971] data plotted as *Zo*/*h* against λ as originally calculated by *Marticorena and Bergametti* [1995] in comparison to its correct value. (bottom) *Marshall* [1971] data modeled by f_{eff} plotted against its measured SSR showing the difference in the value of a = 0.35 and a = 0.70. The prediction by the *Raupach* [1994] model of *Marshall* [1974] is plotted for comparison.

however their performance when tested in a field environment is less favorable. The *Marticorena and Bergametti* [1995] model seems to display a scaling dependency when the difference between z_{oS} and the overall Z_o is too great, creating a negative partition, having no physical meaning. While the *Raupach et al.* [1993] model requires more inputs than are required by the *Marticorena and Bergametti* [1995] model, its predictions are better owing

to the incorporation of more variations in the roughness geometry and the alterations to the flow they can cause.

[48] Further comparisons would have been possible if more published data sets had provided more detailed information about their experimental methods and measured aerodynamic properties (i.e., free stream velocity, roughness heights, etc.). In addition, field experiments over sparse canopies may require a spatially averaged logarithmic profile as well as a time-averaged one due to the nonuniform nature of the roughness layer over sparsely vegetated surfaces with large vegetation (greater than one meter). Theoretically, this can also be achieved when the direction of the wind is maintained within a narrow degree window that does not significantly vary over the averaging time period.

[49] The findings of this paper detailing the performance of these two partition based wind erosion models reinforces the need for semiempirical approaches to modeling but also reflects the requirement for more experimental results to develop the models. Furthermore, the implications for the predictive capacity of wind erosion models for vegetated areas seem promising when the right information is available.

Appendix A

[50] This section documents the error found in the work of *Marticorena and Bergametti* [1995] for the calculation of f_{eff} for the data set of *Marshall* [1971] and presents an alternative solution for f_{eff} that is used in the manuscript to analyze the model's performance.

[51] *Marshall*'s [1971] data set is from a laboratory wind tunnel study that made shear stress measurements on individual cylindrical roughness elements of different sizes with a steady free stream velocity of 20.3 m s^{-1} measured at a height of 0.28 m. Measurements were tabulated within his manuscript allowing for the calculation of total shear stress (τ) and surface shear stress (τ_s) with corresponding roughness densities (λ). We used the 'law of the wall' to calculate Z_o for *Marshall*'s [1971] roughness arrays and his tabulated surface stress values for the surface with no elements with its associated free stream wind speed to calculate z_{oS}.

[52] *Marticorena and Bergametti* [1995] similarly used the *Marshall* [1971] data set to calculate Z_o and z_{oS} but used a free stream velocity of 20.3 m/s at a height of 0.046 m in error (B. Marticorena, personal communication, 2003). This produces values an order of magnitude lower for Z_o but does not change the value of z_{oS}. This greatly affects the Z_o/h and λ relationship used to produce the roughness regression of *Marticorena et al.* [1997] for predicting Z_o (Figure A1, top).

[53] The *Elliot* [1958] solution for the a term disagrees with the one provided by *Pendergrass and Arya* [1984] and used by *Marticorena and Bergametti* [1995]. Equation 10 shows that a is a function of the roughness density and wind flow properties and is calculated using Z_o and z_{oS} of the surface. The average value for a using the *Elliot* [1958] solution for the *Marshall* [1971] data set is 0.7 (standard deviation of 0.06), which doubles the value of 0.35 proposed by *Pendergrass and Arya* [1984]. Although an average value of a is given as a solution it is apparent that for the same underlying surface (z_{oS} stays constant) there will be a distribution of a values based on changes in roughness density.

[54] Comparing the measured to modeled f_{eff} values while using $a = 0.7$ for the *Marshall* [1971] data set the standard error is 2% lower than when using the *Marticorena and Bergametti* [1995] suggested value of 0.35 (Figure A1, bottom). When using $a = 0.35$ to compare the measured and modeled laboratory wind tunnel tests (Figure 5) the slope slightly decreases to a value of 1.01 but the regression coefficient decreases to 0.88 (with an increase in the standard error by 2%) from 0.90. When f_{eff} is solved with $a = 0.35$ instead of 0.70 for all the data sets (wind tunnel and field studies) used in the model comparison the regression coefficient decreases to 0.54 (from 0.67 for $a = 0.7$) while the standard error increases by 7%.

[55] On the basis of the above analyses, we conclude that $a = 0.7$ provides a better solution than the value used by *Marticorena and Bergametti* [1995] for the f_{eff} function (equation (11)).

Notation

- a surface concentration geometric and flow property parameter.
- b roughness element width (m).
- C_R element drag coefficient.
- C_S surface drag coefficient.
- d displacement height (m).
- f_{eff} shear velocity ratio [*Marticorena and Bergametti*, 1995].
- h roughness element height (m).
- m surface shear stress inhomogeneity parameter.
- n number of roughness elements.
- R_t threshold shear velocity; threshold shear stress ratio [*Raupach*, 1992].
- R_t' threshold shear velocity; threshold shear stress ratio [*Raupach et al.*, 1993].
- R_t'' maximum shear velocity; shear stress ratio [*Raupach et al.*, 1993].
- S surface area occupied by roughness elements (m^2).
- u_z mean wind speed at height z (m s^{-1}).
- u_* shear velocity (m s^{-1}).
- u_{*S} small-scale shear velocity on intervening area among roughness elements (m s^{-1}).
- x distance downwind from an individual roughness element (m).
- z height above the surface (m).
- Z_o roughness length (m).
- z_{oS} local aerodynamic roughness length of the intervening surface (m).
- β ratio of roughness element to surface drag coefficients.
- δ internal boundary layer height (m).
- κ von Karman constant (0.4).
- λ surface roughness concentration.
- ρ_a air density (kg m^{-3}).
- σ ratio of element basal to frontal area.
- τ shear stress (N m^{-2}).
- τ_s surface shear stress (N m^{-2})
- τ_s' mean surface shear stress acting on intervening area among roughness elements (N m^{-2}).

τ_s'' maximum surface shear stress acting on intervening area among roughness elements (N m^{-2}).

[56] **Acknowledgments.** J. King and W. G. Nickling acknowledge funding support from the Natural Sciences and Engineering Research Council, Canada. Funding from the U.S. National Science Foundation (grant 9972960) and financial support from the Division of Atmospheric Sciences, Desert Research Institute, to J. A. Gillies is gratefully acknowledged. This material is based, in part, upon work supported by the Cooperative State Research, Education, and Extension Service, U.S. Department of Agriculture, under agreement 00-35101-9310. Any opinions, findings, conclusions or recommendations expressed in this publication are those of the authors and do not necessarily reflect the view of the U.S. Department of Agriculture. We would also like to thank the University of Guelph undergraduate students for helping with the wind tunnel study.

References

Alfaro, S. C., and L. Gomes (1995), Improving the large-scale modeling of the saltation flux of soil particles in presence of nonerodible elements, *J. Geophys. Res.*, *100*(D8), 16,357–16,366.

Arya, S. P. S. (1975), A drag partition theory for determining the large-scale roughness parameter and wind stress on the arctic pack ice, *J. Geophys. Res.*, *80*(24), 3447–3454.

Castro, I. P. (1971), Wake characteristics of two-dimensional perforated plates normal to an air-stream, *J. Fluid Mech.*, *46*, 599–609.

Coles, D. (1956), The law of the wake in the turbulent boundary layer, *J. Fluid Mech.*, *1*, 191–226.

Crawley, D. M. (2000), A wind-tunnel investigation of drag partition, MSc. thesis, Univ. of Guelph, Guelph, Ont., Canada.

Crawley, D. M., and W. G. Nickling (2003), Drag partition for regularly-arrayed rough surfaces, *Boundary Layer Meteorol.*, *107*, 445–468.

Elliot, W. P. (1958), The growth of the atmospheric internal boundary layer, *Eos Trans. AGU*, *39*(6), 1048–1054.

Finnigan, J. J. (1979), Turbulence in waving wheat I. Mean statistics and honami, *Boundary Layer Meteorol.*, *16*, 181–211.

Garratt, J. R. (1977), Aerodynamic roughness and mean monthly surface stress over Australia, *Div. Atmos. Phys. Tech Pap. 29*, Commonw. Sci. and Ind. Res. Organ., Canberra.

Garratt, J. R. (1980), Surface influence upon vertical profiles in the atmospheric near surface layer, *Q. J. R. Meteorol.*, *Soc.,106*, 803–819.

Gillette, D. A., and P. H. Stockton (1989), The effect of nonerodible particles on wind erosion of erodible surfaces, *J. Geophys. Res.*, *94*, 12,885–12,893.

Gillette, D. A., G. Herbert, P. H. Stockton, and P. R. Owen (1996), Causes of the fetch effect in wind erosion, *Earth Surf. Processes Landforms*, *21*(7), 641–660.

Gillies, J. A., N. Lancaster, W. G. Nickling, and D. M. Crawley (2000), Field determination of drag forces and shear stress partitioning effects for a desert shrub (*Sarcobatus vermiculatus*, greasewood), *J. Geophys. Res.*, *105*, 24,871–24,880.

Gillies, J. A., W. G. Nickling, and J. King (2002), Drag coefficient and plant form-response to wind speed in three plant species: Burning bush (*Euonymus alatus*), Colorado blue spruce (*Picea pungens glauca.*), and fountain grass (*Pennisetum setaceum*), *J. Geophys. Res.*, *107*(D24), 4760, doi:10.1029/2001JD001259.

Glendening, J. W. (1977), Aeolian transport and vegetative capture of particles, M.Sc. thesis, Colorado State Univ., Fort Collins.

Hagan, L. J., and L. Lyles (1988), Estimating small grain equivalents of shrub-dominated rangelands for wind erosion control, *Tran. ASAE*, *31*(3), 769–775.

Jackson, P. S. (1981), On the displacement height in the logarithmic profile, *J. Fluid Mech.*, *111*, 15–25.

Jarvis, P. G., G. B. James, and J. J. Landsberg (1976), Coniferous forest, in *Vegetation and the Atmosphere*, edited by J. L. Monteith, pp. 171–240, Elsevier, New York.

Kim, D. S., G. H. Cho, and B. R. White (2000), A wind-tunnel study of atmospheric boundary-layer flow over vegetated surfaces to suppress PM10 emission on Owens (dry) Lake, *Boundary Layer Meteorol.*, *97*, 309–329.

Kutzbach, J. (1961), Investigations of the modification of wind profiles by artificially controlled surface roughness, in *Studies of the Three Dimensional Structure of the Planetary Boundary Layer*, annual report, pp. 71–113, Dep. of Meteorol., Univ. of Wis., Madison.

Lancaster, N., and A. Baas (1998), Influence of vegetation cover on sand transport by wind: Field studies at Owens Lake, California, *Earth Surf. Processes Landforms*, *23*(1), 69–82.

Lee, B. E., and B. F. Soliman (1977), An investigation of the forces on three dimensional bluff bodies in rough wall turbulent boundary layers, *J. Fluids*, 503–510.

Lettau, H. (1969), Note on aerodynamic roughness-parameter estimation on the basis of roughness-element description, *J. Appl. Meteorol.*, *8*, 828–832.

Luttmer, C. (2002), The partition of drag in salt grass communities, M.Sc. thesis, Univ. of Guelph, Guelph, Ont., Canada.

Lyles, L., and B. E. Allison (1975), Wind erosion: The protective role of simulated standing stubble, *Am. Soc. Agric. Eng.*, *19*(1), 61–64.

MacKinnon, D. J., G. D. Clow, R. K. Tigges, R. L. Reynolds, and P. S. Chavez Jr. (2004), Comparison of aerodynamically and model-derived roughness lengths (z_o) over diverse surfaces, central Mojave Desert, California, USA, *Geomorphology*, *63*, 103–113.

Marshall, J. K. (1971), Drag measurements in roughness arrays of varying densities and distribution, *Agric. Meteorol.*, *8*, 269–292.

Marticorena, B., and G. Bergametti (1995), Modeling the atmospheric dust cycle: 1. Design of a soil-derived dust emission scheme, *J. Geophys. Res.*, *100*, 16,415–16,430.

Marticorena, B., G. Bergametti, B. Aumont, Y. Callot, C. N'Doumé, and M. Legrand (1997), Modeling the atmospheric dust cycle: 2. Simulation of Saharan dust sources, *J. Geophys. Res.*, *102*, 4387–4404.

Minvielle, F., B. Marticorena, D. A. Gillette, R. E. Lawson, R. Thompson, and G. Bergametti (2003), Relationship between the aerodynamic roughness length and the roughness density in cases of low roughness density, *J. Fluid Mech. Eng.*, *3*, 249–267.

Musick, H. B., and D. A. Gillette (1990), Field evaluation of relationships between a vegetation structural parameter and sheltering against wind erosion, *Land Degrad. Rehabil.*, *2*, 87–94.

Musick, H. B., S. M. Trujillo, and C. R. Truman (1996), Wind-tunnel modelling of the influence of vegetation structure on saltation threshold, *Earth Surf. Processes Landforms*, *21*(7), 589–605.

Nickling, W. G., N. Lancaster, and J. A. Gillies (1997), Field wind tunnel studies of relations between vegetation cover and dust emissions at Owens Lake, report, 30 pp., Great Basin Unified Air Pollut. Control Dist., Bishop, Calif.

Nickling, W. G., J. A. Gillies, N. Lancaster, and D. M. Crawley (1999), Optimizing managed vegetation planting configurations at Owens Lake, California, report, 75 pp., Great Basin Unified Air Pollut. Control Dist., Bishop, Calif.

Panofsky, H. A., and A. A. Townsend (1964), Change of terrain roughness and the wind profile, *Q. J. R. Meteorol. Soc.*, *90*, 147–155.

Pendergrass, W., and S. P. S. Arya (1984), Dispersion in neutral boundary layer over a step change in surface roughness, I, Mean flow and turbulence structure, *Atmos. Environ.*, *18*, 1267–1279.

Priestley, C. H. B. (1959), *Turbulent Transfer in the Lower Atmosphere*, 130 pp., Univ. of Chicago Press, Chicago, Ill.

Raupach, M. R. (1992), Drag and drag partition on rough surfaces, *Boundary Layer Meteorol.*, *60*, 375–395.

Raupach, M. R. (1994), Simplified expressions for vegetation roughness length and zero-plane displacement as functions of canopy height and leaf area index, *Boundary Layer Meteorol.*, *71*, 211–216.

Raupach, M. R., A. S. Thom, and I. Edwards (1980), A wind-tunnel study of turbulent flow close to regularly arrayed rough surfaces, *Boundary Layer Meteorol.*, *18*, 373–397.

Raupach, M. R., D. A. Gillette, and J. F. Leys (1993), The effect of roughness elements on wind erosion threshold, *J. Geophys. Res.*, *98*, 3023–3029.

Schlichting, H. (1936), Experimentelle untersuchungen zum Rauhigkeitsproblem, *Ing. Arch.*, *7*, 1–34.

Shao, Y., and L. M. Leslie (1997), Wind erosion prediction over the Australian continent, *J. Geophys. Res.*, *102*, 30,091–30,105.

Stout, J. E., and T. M. Zobeck (1997), Intermittent saltation, *Sedimentology*, *44*(5), 959–970.

Sullivan, R., and R. Greeley (1993), Comparison of aerodynamic roughness measured in a field experiment and in a wind tunnel simulation, *J. Wind Eng. Ind. Aerodyn.*, *48*, 25–50.

Taylor, P. A. (1988), Turbulent wakes in the atmospheric boundary layer, in *Flow and Transport in the Natural Environment: Advances and Application*, edited by W. L. Steffen and O. T. Denmead, pp. 270–292, Springer, New York.

Tegen, I., P. Harrison, K. Kohfeld, I. C. Prentice, M. Coe, and M. Heimann (2002), Impact of vegetation and preferential source areas on global dust aerosol: Results from a model study, *J. Geophys. Res.*, *107*(D21), 4576, doi:10.1029/2001JD000963.

Thom, A. S. (1971), Momentum absorption by vegetation, *Q. J. R.. Meteorol. Soc.*, *97*, 414–428.

Wieringa, J. (1993), Representative roughness parameters for homogenous terrain, *Boundary Layer Meteorol.*, *63*, 323–363.

Wolfe, S. A., and W. G. Nickling (1993), The protective role of sparse vegetation in wind erosion, *Prog. Phys. Geogr.*, *17*(1), 50–68.

Wolfe, S. A., and W. G. Nickling (1996), Shear stress partitioning in sparsely vegetated desert canopies, *Earth Surf. Processes Landforms*, *21*, 607–619.

Woodell, S. R. J., H. A. Mooney, and A. J. Hill (1969), The behaviour of *Larrea divaricata* (creosote bush) in response to rainfall in California, *J. Ecol.*, *57*(1), 37–44.

Wyatt, V. E., and W. G. Nickling (1997), Drag and shear stress partitioning in sparse desert creosote communities, *Can. J. Earth Sci.*, *34*, 1486–1498.

Zender, C., H. Bian, and D. Newman (2003), Mineral Dust Entrainment and Deposition (DEAD) model: Description and 1990s dust climatology, *J. Geophys. Res.*, *108*(D14), 4416, doi:10.1029/2002JD002775.

J. A. Gillies, Particle Emissions Measurement Laboratory, Division of Atmospheric Sciences, Desert Research Institute, 2215 Raggio Parkway, Reno, NV 89512, USA. (jackg@dri.edu)

J. King and W. G. Nickling, Wind Erosion Laboratory, Department of Geography, University of Guelph, Guelph, ON Canada, N1G 2W1.